NUCLEAR SCIENCE AND ENGINEERING · VOLUME 183 · 371–386 · JULY 2016

Total Uncertainty Analysis for PWR Assembly Based on the Statistical Sampling Method

Tiejun Zu,[a] Chenghui Wan,[a] Liangzhi Cao,[a]* Hongchun Wu,[a] and Wei Shen[a,b]

[a]*Xi'an Jiaotong University, School of Nuclear Science and Technology, 28 West Xianning Road, Xi'an, Shaanxi 710049, China*
[b]*Canadian Nuclear Safety Commission, K1P 5S9, Ottawa, Ontario, Canada*

Received September 19, 2015
Accepted for Publication February 6, 2016
http://dx.doi.org/10.13182/NSE15-96

Abstract — *The nuclear-data uncertainties impact the best-estimate predictions of the nuclear reactor system. In this paper, total uncertainty analyses have been performed for the TMI-1 assembly at both hot zero-power and hot full-power conditions to evaluate the impacts of nuclear-data uncertainties on the predictions of lattice calculations, based on the statistical sampling method. With an improved multigroup cross-section perturbation model, the contributions of various basic cross sections to the uncertainties of k_∞ and two-group macroscopic cross sections are obtained. For the total uncertainty analyses, a 172-group cross-section covariance library produced from ENDF/B-VII.1 is used to generate the samples for the multigroup microscopic cross-section library, and DRAGON 5.0 is applied to perform lattice calculations for each sample. The numerical results show that the relative uncertainty of k_∞ can reach about 4.7‰ using the ν_p covariance matrix of ^{235}U-ν and 7.1‰ using the ν_t covariance matrix of ^{235}U-ν. The relative uncertainties of two-group macroscopic cross sections vary from about 2.9‰ (for the total cross section of the thermal group) to about 11.9‰ (for the scattering cross section from the fast group to the thermal group). Moreover, through detailed analysis toward uncertainty origins, it has been observed that ^{235}U, ^{238}U, ^{16}O, and ^{1}H are the four most significant contributors, and the uncertainties of ^{235}U-(ν, σ_f, σ_γ), ^{238}U-(σ_γ, $\sigma_{(n,inel)}$, $\sigma_{(n,elas)}$, ν), ^{16}O-($\sigma_{(n,elas)}$), and ^{1}H-($\sigma_{(n,elas)}$, σ_γ) are the most significant cross-section contributors.*

Keywords — *Total uncertainty analysis, nuclear-data uncertainties, statistical sampling method.*

Note — *Some figures may be in color only in the electronic version.*

I. INTRODUCTION

The Organisation for Economic Cooperation and Development/Nuclear Energy Agency has organized the Uncertainty Analysis in Modeling (UAM) expert group to satisfy the increasing demands for best-estimate predictions to be provided with their confidence bounds in many domains, including nuclear research, industry, safety, and regulation.[1] The objective of UAM is to quantify the uncertainties for system prediction results for light water reactors, propagating the uncertainty sources through different scales and physics phenomena, including the neutronics phase, core phase, and system phase. Recently, the lack of precision of the nuclear data has been treated as one of the most significant sources of uncertainty for the responses of neutronics calculations.[2] Therefore, the objectives of the neutronics phase proposed by UAM are aimed at propagating the multigroup microscopic cross-section uncertainties through the neutronics calculations and determining the uncertainties of the few-group macroscopic cross section for the lattice physics and the uncertainties of the core steady-state stand-alone neutronics predictions for the core physics. In this context, in recent years, uncertainty analysis has been focused on propagating the nuclear-data uncertainties to the responses of neutronics calculations. By applying

*E-mail: caolz@mail.xjtu.edu.cn

uncertainty analysis for neutronics calculations, the confidence bounds of the neutronics prediction results can be quantified, and therefore, much more reliable and confident predictions can be provided.

According to previous research on propagating the nuclear-data uncertainties to the responses of neutronics calculations, the proposed schemes can be classified into two groups: the explicit scheme and the total scheme.[3] This classification is because in the deterministic neutronics calculation method, both the resonance self-shielding calculation and the neutron-transport calculation are required. The explicit scheme is first proposed, aimed at determining the uncertainties of neutronics responses introduced by the uncertainties of effective self-shielding cross sections through only the neutron-transport calculation directly. In this case, the effects of microscopic cross sections on the effective self-shielding cross sections through the resonance self-shielding calculation, which is defined as the implicit effects, are ignored. As an improvement, the total uncertainty analysis scheme[4–7] has been proposed. This considers the resonance self-shielding effects and is defined as the summation of the explicit and implicit effects. The total uncertainty analysis scheme can propagate the multigroup microscopic cross-section uncertainties to the neutronics responses completely, which satisfies the requirements of the uncertainty analysis proposed by UAM for the neutronics phase. In this context, the total uncertainty analysis scheme has been adopted in this paper.

To perform a total uncertainty analysis for neutronics calculations, there are two widely applied categories of methodologies: the deterministic method and the statistical sampling method. For the deterministic method, the sensitivity analysis is performed first to obtain the relative sensitivity coefficients of responses with respect to the multigroup cross sections, and then the uncertainties of responses are calculated using the first-order uncertainty propagation rule, the sandwich rule.[2] For the statistical sampling method,[8] samples of multigroup cross-section libraries are first generated according to the covariance matrices of the cross sections. These samples of the multigroup cross-section libraries are then provided to the lattice code for the resonance self-shielding and neutron-transport calculations, and the corresponding neutronics responses are obtained. Finally, the covariance matrices of the responses, containing the uncertainty information of the responses, can be computed by the statistical calculation method. Compared with the deterministic method, the statistical sampling method has some notable advantages.[9] For this method, there is no approximation to the uncertainty results, while a first-order approximation is applied by the deterministic method. Moreover, there is no special treatment for different responses for the statistical sampling method, while for the deterministic methods based on perturbation theory, different perturbation models should be established for different responses.[10] In this context, the statistical sampling method is much more capable and therefore has been adopted to perform the total uncertainty analysis in this paper.

A new functional code, named UNICORN, has been developed in our research group to perform total uncertainty analysis for neutronics calculations, applying the statistical sampling method. In this code, an improved multigroup cross-section perturbation model and consistency rules for both integral and basic cross sections have been established and implemented, which make it capable of analyzing much more detailed uncertainty origin information. The uncertainty analysis capability for the basic cross sections is important, because it can provide much more detailed uncertainty origin information, which is essential and significant for determining the main uncertainty sources and performing a deeper analysis. With this improved multigroup cross-section perturbation model, a total uncertainty analysis can be performed not only for the integral cross sections, containing σ_t, σ_a, and σ_s, but also for the basic cross sections, including $\sigma_{(n,elas)}$, $\sigma_{(n,inel)}$, $\sigma_{(n,2n)}$, $\sigma_{(n,3n)}$, σ_f, σ_γ, $\sigma_{(n,p)}$, $\sigma_{(n,\mathrm{D})}$, $\sigma_{(n,\mathrm{T})}$, $\sigma_{(n,\mathrm{He})}$, $\sigma_{(n,\alpha)}$, and ν. Moreover, an improvement to the statistical sampling method, the bootstrap method[11] has been applied in UNICORN to give much more confident and reliable uncertainty results. In addition, the lattice code DRAGON 5.0 (Ref. 12) has been applied by the UNICORN code to carry out the resonance self-shielding and neutron-transport calculations, by applying the WIMSD-4 format multigroup microscopic cross-section library.[13]

The contents of the following three sections are as follows. In Sec. II, we provide an overview of the UNICORN code for total uncertainty analysis and introduce the fundamental theory and the statistical sampling method. Section III shows the uncertainty results and a detailed analysis of the origin uncertainty information for the TMI-1 assembly at both the hot zero-power (HZP) and hot full-power (HFP) conditions. Conclusions drawn from this work are discussed in Sec. IV.

II. OVERVIEW

In this paper, the home-developed UNICORN code[14] is applied to perform the total uncertainty analyses for the TMI-1 assembly at both HZP and HFP conditions to quantify the uncertainties of the neutronics responses introduced by the multigroup microscopic cross-section uncertainties. In our previous work, the theory of the sampling method for the response uncertainty calculation

was limited to only one response. It has been extended to multiple responses and the theories for the sampling method are a little different. Therefore, the theory used in this paper is introduced briefly to characterize the difference. More detailed theory and methods applied in this code can be found in our previous work.[14]

A flowchart of the UNICORN code for total uncertainty analysis is shown in Fig. 1.

II.A. Essential Nuclear Data

As shown in Fig. 1, the nuclear data are the essential and prerequisite element for total uncertainty analysis by the UNICORN code, because the samples of multigroup microscopic cross-section libraries are generated based on these nuclear data. The nuclear data consist of not only the integral cross sections, including σ_t, σ_s, and σ_a, but also the basic cross sections, containing $\sigma_{(n,elas)}$, $\sigma_{(n,inel)}$, $\sigma_{(n,2n)}$, $\sigma_{(n,3n)}$, σ_f, σ_γ, $\sigma_{(n,p)}$, $\sigma_{(n,D)}$, $\sigma_{(n,T)}$, $\sigma_{(n,He)}$, $\sigma_{(n,\alpha)}$, and ν. In this paper, the nuclear data have two different sources. First, the integral and some basic cross sections are contained in the WIMSD-4 format multigroup microscopic cross-section library, including σ_{tr}, σ_s, σ_a, σ_f, and $\nu\sigma_f$, and

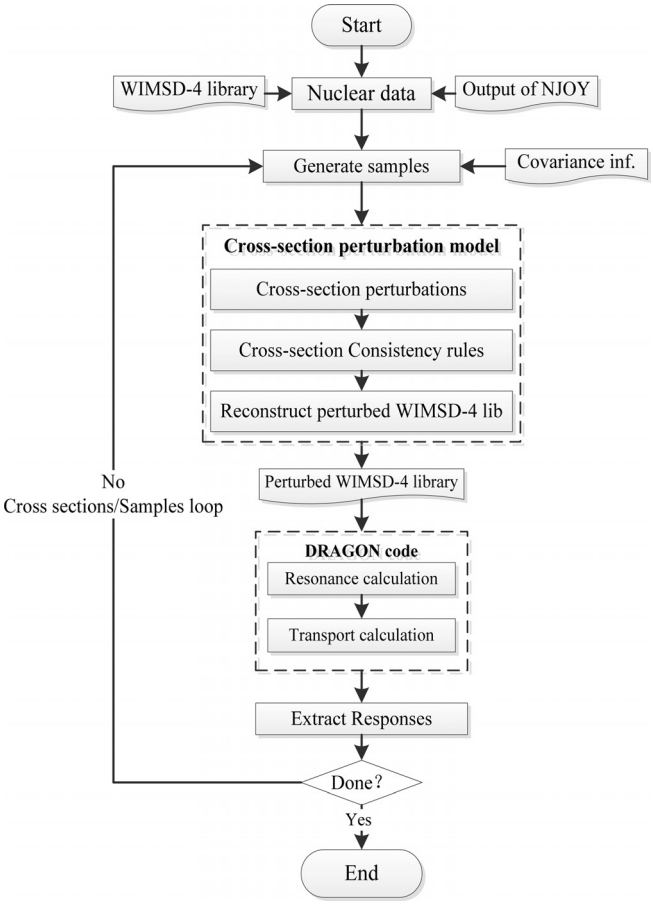

Fig. 1. Flowchart of the UNICORN code.

corresponding resonance integral information, which are directly read from the WIMSD-4 format library. The NJOY code is used to generate the WIMSD-4 format library. Second, some other basic cross sections, including $\sigma_{(n,inel)}$, $\sigma_{(n,2n)}$, $\sigma_{(n,3n)}$, $\sigma_{(n,p)}$, $\sigma_{(n,D)}$, $\sigma_{(n,T)}$, $\sigma_{(n,He)}$, and $\sigma_{(n,\alpha)}$, which are not contained in the WIMSD-4 format library, are converted from the output files of NJOY (Ref. 15). $\sigma_{(n,elas)}$ and σ_γ are contained in neither the WIMSD-4 library nor the NJOY output files. Therefore, based on the cross sections contained in the WIMSD-4 library and the output files of NJOY, $\sigma_{(n,elas)}$ and σ_γ are obtained by the application of the cross-section consistency rules,[13] which can be characterized as

$$\sigma_{(n,elas),g\to h} = \sigma_{s,g\to h} - \sigma_{(n,inel),g\to h} - 2\sigma_{(n,2n),g\to h} - 3\sigma_{(n,3n),g\to h} \quad (1)$$

and

$$\sigma_{\gamma,g} = \sigma_{a,g} + \sigma_{(n,2n),g} + 2\sigma_{(n,3n),g} - \sigma_{f,g} - \sigma_{(n,p)} - \sigma_{(n,D)} - \sigma_{(n,T)} - \sigma_{(n,He)} - \sigma_{(n,\alpha)} - \sigma_{(n,2\alpha)} . \quad (2)$$

In Eqs. (1) and (2), the scattering and absorption cross sections for the g'th group are modified to preserve the neutron balance by correcting $\sigma_{(n,2n)}$ and $\sigma_{(n,3n)}$ according to the WIMSD-4 format multigroup microscopic cross-section library. Equations (1) and (2) can be applied as cross-section consistency rules to keep the cross-section balance. On the right side of Eq. (1), the scattering cross section σ_s can be obtained from the WIMSD-4 library or the NJOY output files. The other basic cross sections are all from the output file of NJOY. For the right-side cross sections in Eq. (2), σ_a and σ_f are from the WIMSD-4 library, and the other basic cross sections are from the NJOY output file. For σ_a and σ_f within the resonance groups (e.g., the 46th to 92nd groups for the 172-group energy structure), the resonance cross sections should be converted from the corresponding resonance integrals contained in the WIMSD-4 format multigroup microscopic cross-section library, using the relationship

$$\sigma_{x,g}(T,\sigma_b) = \frac{I_{x,g}(T,\sigma_b)\sigma_b}{\sigma_b - I_{a,g}(T,\sigma_b)} , \quad (3)$$

where σ_b is defined as the background cross section; $\sigma_{x,g}(T,\sigma_b)$ and $I_{x,g}(T,\sigma_b)$ represent the resonance absorption cross section and resonance integral of type x, respectively, at temperature T and background cross section σ_b. In Eq. (3), the resonance integral $I_{x,g}(T,\sigma_b)$ can represent $I_{a,g}(T,\sigma_b)$ and $I_{\nu f,g}(T,\sigma_b)$ for the σ_a and $\nu\sigma_f$ resonance integrals, correspondingly. By applying Eq. (3), the tables of resonance integrals, contained in the WIMSD-4 format

library, can be converted to tables of resonance cross sections, and vice versa.

Based on the methods described above, the essential nuclear data for the total uncertainty analysis can be completely obtained by application of the data from the WIMSD-4 libraries and NJOY output files, and the multigroup cross-section consistency rules in Eqs. (1) and (2).

II.B. Samples for the Cross Sections

The generation of samples for the multigroup microscopic cross-section libraries is the most significant part that UNICORN performs in a total uncertainty analysis using the statistical sampling method. Actually, the generation of the cross-section samples is the process that perturbs the multigroup microscopic cross sections near their expectation values within the distribution ranges, determined by the multigroup cross-section uncertainties. Therefore, an improved multigroup cross-section perturbation model is established and applied in the UNICORN code, which can perform cross-section perturbations for both the integral and basic multigroup microscopic cross sections mentioned above and consequently generate the cross-section samples. A more detailed introduction to the improved multigroup cross-section perturbation model and sample generation for multigroup cross-section libraries is in our previous work.[14]

As per the foregoing descriptions, only the integral cross sections, including σ_{tr}, σ_s, σ_a, and some basic cross sections, including σ_f and $\nu\sigma_f$, are contained in the WIMSD-4 format multigroup microscopic cross-section library, because these cross sections are essential and sufficient for the resonance self-shielding and neutron-transport calculations. When an uncertainty analysis is performed for the other basic cross sections, which are excluded in the WIMSD-4 library (e.g., $\sigma_{(n,inel)}$, $\sigma_{(n,2n)}$, $\sigma_{(n,3n)}$, etc.), the consistency rules for the integral and basic cross sections, which are shown in Eqs. (1) and (2), should be applied to keep the essential integral and basic cross-section balance to ensure the successful and correct execution of the lattice code. For example, when an uncertainty analysis is performed for the $\sigma_{(n,inel)}$ cross section, both the scattering and total cross sections are not sampled and just changed to the corresponding values, according to the samples of the $\sigma_{(n,inel)}$ cross section. Moreover, for the resonant cross sections within the resonance groups, such as $\nu\sigma_f$, the cross-section samples should be converted to the essential table format of resonance integrals by applying Eq. (3). With the sample information for the multigroup microscopic cross-section libraries, a newly sampled or perturbed WIMSD-4 format multigroup microscopic cross-section library is reconstructed and converted to binary format.

Finally, the perturbed binary WIMSD-4 format multigroup microscopic libraries are provided to the DRAGON 5.0 code to execute the resonance self-shielding and neutron-transport calculations. The corresponding responses can be obtained, and then provided to the statistical calculations to quantify the uncertainties of the responses for the neutronics calculations.

II.C. Theory of the Statistical Sampling Method

The statistical sampling method has been adopted and implemented in the UNICORN code for the total uncertainty analysis. In this section, the basic theory and methods of the statistical sampling method are introduced.

For any multi-input and multiresponse system, the relationship of the responses and inputs can be briefly characterized as

$$\boldsymbol{R} = \boldsymbol{f}(\boldsymbol{X}) , \tag{4}$$

where $\boldsymbol{X}$ represents the multi-input vector and can be characterized as $\boldsymbol{X} = [x_1, x_2, \ldots, x_{nX}]^T$ in which nX is the number of input parameters. $\boldsymbol{R}$ represents the multiresponse vector and can be characterized as $\boldsymbol{R} = [R_1, R_2, \ldots, R_{nR}]^T$ in which nR is the number of responses.

To propagate the uncertainties of the input parameters to the responses, three main steps[8] are performed: first, determine the distribution ranges of the input parameters; second, generate the samples of the input parameters according to the input-parameter distribution ranges; finally, execute the system calculations using the samples of the input parameters, and quantify the uncertainties of the interested responses, with the responses obtained by all input samples.

In the first step, the distribution ranges of the input parameters are required. The uncertainties of the input parameters are essential to determine the input distribution ranges. The covariance matrix of the input parameters $\boldsymbol{X}$ can be defined as $\boldsymbol{\Sigma}$, in which the diagonal elements present the variances or uncertainties of the input parameters, and the off-diagonal elements are the covariance or correlations between different input parameters. Combined with the expectation vector $\boldsymbol{\mu}$, which can be characterized as $\boldsymbol{\mu} = [\mu_1, \mu_2, \ldots, \mu_{nX}]^T$, the distribution ranges of each input parameter can be determined. In this paper, for the neutronics calculations, the input parameters $\boldsymbol{X}$ are the multigroup microscopic cross sections. The corresponding expectation vector $\boldsymbol{\mu}$ represents the multigroup microscopic cross section contained in the library, which is generated from the ENDFs. The covariance

matrix $\boldsymbol{\Sigma}$ of the multigroup cross sections can also be produced from the ENDFs (Ref. 16).

In the second step, the samples of the input parameters are generated according to the distribution ranges of the input parameters. By application of the covariance matrix $\boldsymbol{\Sigma}$ and expectation vector $\boldsymbol{\mu}$, the samples of the input parameters can be generated as

$$\boldsymbol{X}_S = \sum^{1/2} \boldsymbol{Y}_S + \boldsymbol{\mu} , \tag{5}$$

where $\boldsymbol{X}_s$ represents the sample for $\boldsymbol{X}$. $\boldsymbol{Y}_s$ represents the sample for $\boldsymbol{Y}$, which has the same dimension as $\boldsymbol{X}$. All the parameters of $\boldsymbol{Y}$ are independent and obey the standard normal distributions. $\boldsymbol{\Sigma}^{1/2}$ is the square root of covariance $\boldsymbol{\Sigma}$. It is quite practical and convenient to generate the samples $\boldsymbol{Y}_s$ for independent parameters $\boldsymbol{Y}$, based on which the samples $\boldsymbol{X}_s$ for dependent parameters $\boldsymbol{X}$ can be obtained according to Eq. (5).

Finally, all the samples of the input parameters are used in the system calculations to obtain the corresponding responses, based on which the response uncertainties can be computed. The i'th sample of the input parameters $\boldsymbol{X}_{s,i}$ ($i = 1, 2, \ldots, nS$, where nS is the number of samples), which can be characterized as $\boldsymbol{X}_{s,i} = [x_{1,i}, x_{2,i}, \ldots, x_{nX,i}]^T$, is used in the system calculation. Thus, the corresponding response vector $\boldsymbol{R}_i$ ($i = 1, 2, \ldots, nS$), which can be characterized as $\boldsymbol{R}_i = [R_{1,i}, R_{2,i}, \ldots, R_{nR,i}]^T$, can be obtained. Therefore, the samples of the input parameters and responses $[\boldsymbol{X}_{s,i}, \boldsymbol{R}_i]$ (for $i = 1, 2, \ldots, nS$) can be obtained. The covariance matrix, which contains the uncertainties and correlations of the responses, can be computed by application of the statistical calculation as

$$\sum_{\boldsymbol{R},i,j} = \frac{1}{nS - 1} \sum_{n=1}^{nS} (R_{i,n} - R_{i,0})(R_{j,n} - R_{j,0}) , \tag{6}$$

where $\boldsymbol{\Sigma}_{\boldsymbol{R}}$ represents the covariance matrix of responses with a size of $nR \times nR$. $\boldsymbol{\Sigma}_{\boldsymbol{R},i,j}$ is the covariance for the i'th and j'th responses ($i, j = 1, 2, \ldots, nR$). $R_{i,n}$ (or $R_{j,n}$) and $R_{i,0}$ (or $R_{j,0}$) stand for the n'th sample value and expectation value for the i'th (or j'th) response R_i (or R_j). The expectation value for R_i can be characterized as

$$R_{i,0} = \frac{1}{nS} \sum_{n=1}^{nS} R_{i,n} . \tag{7}$$

The standard deviations σ_{Ri} of the responses R_i ($i = 1, 2, \ldots, nR$) can be determined by application of the covariance matrix of responses $\boldsymbol{\Sigma}_{\boldsymbol{R}}$, characterized as

$$\sigma_{Ri} = \sqrt{\sum_{R,i,i}} . \tag{8}$$

By applying these three main steps, the covariance matrix of responses can be obtained, and therefore, the uncertainties of the responses can be determined.

For the statistical sampling method, the selection of a sampling technique is important. There are three different sampling techniques[17]: random sampling (RS), stratified sampling (SS), and Latin hypercube sampling (LHS). Random sampling is the easiest technique for generating samples, with the disadvantage that there is no assurance that the samples will cover all subsets of the distribution space for $\boldsymbol{X}$. Stratified sampling can ensure that the samples cover all subsets of the distribution space but has the disadvantage that the strata and strata probabilities must be determined, which makes it complicated to perform the uncertainty analysis by applying samples with different probabilities. The LHS technique incorporates the desirable features of RS and SS. The implementation of the LHS technique is easier than that of SS because it is not necessary to determine the strata and corresponding probabilities, and each sample has the same probability like RS, which makes it practical and convenient for the uncertainty analysis. Arguably, the LHS technique is one of the best small-sample statistical sampling approaches for uncertainty analysis. Therefore, the LHS technique is adopted and applied to generate samples for multigroup microscopic cross sections in the UNICORN code.

For the statistical sampling method to perform an uncertainty analysis, the number of samples should be determined. According to the work of Wilks,[18] the minimum sample size required can be determined, for a certain coverage and confidence for the outputs, as

$$\sum_{i=0}^{r+m-1} C_n^i (1 - \alpha)^i \alpha^{n-i} \leq 1 - \beta , \tag{9}$$

where r and m represent the number of upper and lower tolerance limits, respectively. n is the number of the samples. α and β stand for the coverage and confidence percentage, respectively. In this paper, for the total uncertainty analysis for the eigenvalue and two-group macroscopic cross sections, with the coverage percentile $\alpha = 95\%$ and confidence $\beta = 95\%$, the minimum number of samples required is 361 (Ref. 16). In this context, for much more reliable uncertainty results, the number of samples is determined as $nS = 500$ in this paper. That is to say, 500 different multigroup microscopic cross-section libraries were generated and applied for the total uncertainty analyses for each type of cross section of all nuclides under analysis.

II.D. Bootstrap Method for Confidence Intervals

Statistical errors are inevitably introduced into the uncertainty results because the number of samples is a specific finite number. To enhance the reliability and confidence of uncertainties results, the bootstrap method was applied to evaluate the confidence intervals for the uncertainty results.[11] The resampling technique is used to evaluate the confidence interval for the uncertainty results of the uncertainty analysis, and a series of resamples are generated for the uncertainty analysis. The standard deviation of R_j obtained by the i'th resamples can be presented as σ_{Rj}^{i} ($i = 1, 2, \ldots, N$) where N is the number of resamples. The bootstrap confidence interval $\Delta\sigma_{Rj}$ can be quantified by

$$\Delta\sigma_{Rj} = \sqrt{\frac{1}{N-1}\sum_{n=1}^{N}(\sigma_{Rj}^{n} - \sigma_{Rj}^{0})^2}\,, \tag{10}$$

where

$\Delta\sigma_{Rj}$ = standard deviation of response standard deviations σ_{Rj} for the response R_j

σ_{Rj}^{n} = standard deviation of response R_j obtained by the n'th resamples

σ_{Rj}^{0} = expectation value of the standard deviation obtained by the N resamples, which can be characterized as

$$\sigma_{Rj}^{0} = \frac{1}{N}\sum_{i=1}^{N}\sigma_{Rj}^{i}\,. \tag{11}$$

By application of Eqs. (10) and (11), the confidence intervals for the response uncertainty results can be quantified and the uncertainty results can be made much more confident and reliable with the limited size of samples.

III. RESULTS

In this section, the UAM pressurized water reactor (PWR) benchmarks, the TMI-1 assembly (15 × 15) at both HZP and HFP conditions, are analyzed by the UNICORN code. A 172-group cross-section covariance library, which contains the nuclear-data uncertainty information, is generated based on ENDF/B-VII.1 and applied to UNICORN for the total uncertainty analyses. The uncertainties of k_∞ and two-group macroscopic cross sections have been obtained. The energy cutoff point for the fast and thermal group is set to 0.625 eV.

III.A. TMI-1 Assembly Specifications

The TMI-1 assembly (15 × 15), proposed by UAM, is a typical PWR benchmark, and the detailed specifications and composition materials are shown in Table I.

According to the material compositions of the TMI-1 assembly, uncertainty analyses were performed for the typical nuclides contained in the materials. The nuclides and corresponding types of cross sections analyzed in this paper are shown in Table II. Ten different nuclides, containing 48 cross sections are analyzed for the TMI-1 assembly, at both HZP and HFP conditions.

TABLE I

TMI-1 Assembly Specifications

Parameter	Value
Fuel assembly dimension	15 × 15
Number of fuel rods per fuel assembly	208
Number of guide tubes per fuel assembly	16
Number of instrumentation tubes per fuel assembly	1
Number of Gd pins per fuel assembly	4
Guide tube outside diameter (mm)	13.462
Guide tube inside diameter (mm)	12.649
Guide tube material	Zircaloy-4
Instrumentation tube outside diameter (mm)	12.522
Instrumentation tube inside diameter (mm)	11.201
Instrumentation tube material	Zircaloy-4
Fuel assembly pitch (mm)	218.11
Gap between fuel assemblies (mm)	1.702
Unit cell pitch (mm)	14.427
Fuel pellet diameter (mm)	9.391
Fuel pellet material	UO_2
Fuel density (g/cm^3)	10.283
Fuel enrichment (wt%)	4.85
Cladding outside diameter (mm)	10.928
Cladding thickness (mm)	0.673
Cladding material/density	Zircaloy-4

TABLE II

Nuclides and Cross Sections Analyzed for Uncertainty Analysis

Nuclide(s)	Types of Cross Section
^{1}H	$\sigma_{(n,elas)}$, σ_{γ}
^{90}Zr, ^{91}Zr, ^{92}Zr, ^{94}Zr, ^{96}Zr	$\sigma_{(n,elas)}$, $\sigma_{(n,inel)}$, $\sigma_{(n,2n)}$, σ_{γ}
^{234}U	$\sigma_{(n,elas)}$, $\sigma_{(n,inel)}$, $\sigma_{(n,2n)}$, σ_{f}, σ_{γ}, ν
^{235}U, ^{238}U	$\sigma_{(n,elas)}$, $\sigma_{(n,inel)}$, $\sigma_{(n,2n)}$, $\sigma_{(n,3n)}$, σ_{f}, σ_{γ}, ν
^{16}O	$\sigma_{(n,elas)}$, $\sigma_{(n,inel)}$, $\sigma_{(n,2n)}$, σ_{γ}, $\sigma_{(n,p)}$, $\sigma_{(n,\alpha)}$

III.B. Uncertainty Results and Analysis

In the total uncertainty analyses for the TMI-1 assembly at both HZP and HFP conditions, the sample size was set to $nS = 500$. For much more reliable and confident uncertainty results, the bootstrap method was applied, and ten different resamples with the same size $nS = 500$ were generated and used to perform the uncertainty analyses in this paper.

It should be noted here that the multigroup covariance matrices for ^{235}U-ν are inconsistent for ν_p (the prompt ν) and ν_t (the total ν). Based on ENDF/B-VII.1, the 172-group covariance matrices of ^{235}U-ν for ν_p and ν_t are compared and shown in Fig. 2. By comparing the covariance matrices for ν_p and ν_t of ^{235}U-ν, it can be observed that these two covariance matrices are not consistent. The difference between the covariance matrices is too large to be explained by ν_d (the delayed ν), because the ν_d contribution to ν_t is only approximately 0.64%. Therefore, both covariance matrices of ν_p and ν_t are applied to perform the uncertainty analyses for the TMI-1 assembly at both HZP and HFP conditions, and the effects of the difference on the final uncertainty results of responses are compared and analyzed numerically in this paper.

The total uncertainty analysis results for k_∞ and the two-group macroscopic cross sections of the TMI-1 assembly at both HZP and HFP conditions are shown in Tables III and IV. The only difference in the uncertainty results in Tables III and IV is that the ν_p covariance matrix of ^{235}U-ν is applied for the results in Table III, while the ν_t covariance matrix of ^{235}U-ν is used for the results in Table IV, and the covariance matrices for the other nuclides and cross sections are all the same.

The uncertainty results, shown in Tables III and IV, consist of two parts: the expectation values of the relative uncertainties, represented by $\sigma^0_{Ri}/R_{i,0}$, and the standard deviation of the relative uncertainties, represented by $\Delta\sigma^0_{Ri}/R_{i,0}$. The expectation values and standard deviation of the relative uncertainties are calculated from the ten different resamples. From the uncertainty results, it can be observed that the standard deviations are all within 3% of the expectation values of the corresponding relative uncertainties. This is theoretically reasonable, because according to Wilks,[18] with the sample size $nS = 500$, the response samples would cover over 95% of the distribution ranges with more than 95% confidence, and so do the uncertainty results obtained by the response samples.

From the relative uncertainty results of k_∞ and the two-group macroscopic cross sections of the TMI-1 assembly at both HZP and HFP conditions, three conclusions can be obtained numerically. First, the relative uncertainties of the TMI-1 assembly at HFP conditions are slightly larger than those at HZP conditions. Second, the covariance matrix of ^{235}U-ν notably impacts the uncertainty results of the responses, and the ν_t covariance matrix could introduce larger uncertainties to some

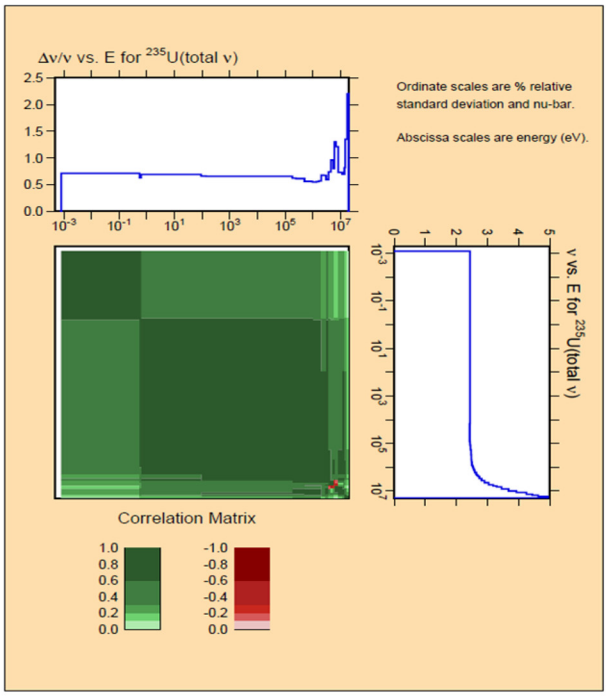

(a)

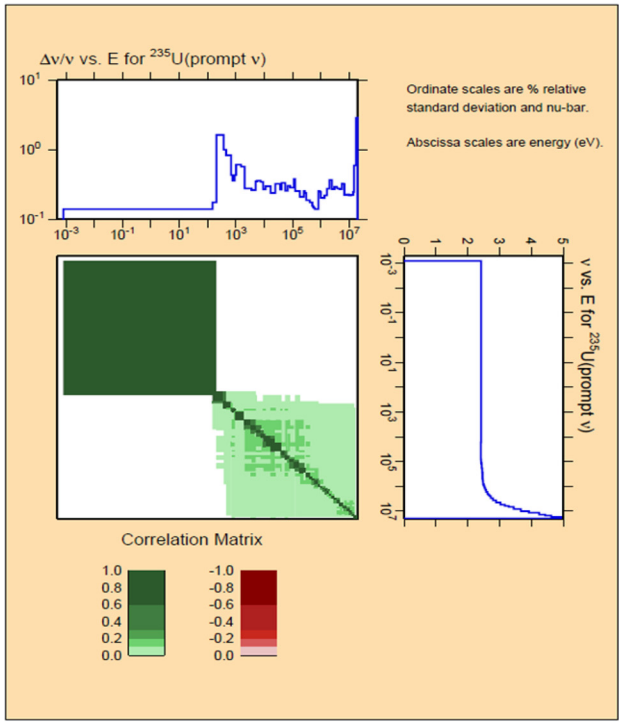

(b)

Fig. 2. Covariance matrices of (a) ^{235}U ν_t and (b) ^{235}U ν_p.

TABLE III

Uncertainties for TMI-1 Assembly Applying ν_p Covariance Matrix of ^{235}U-ν

Response	HZP Conditions		HFP Conditions	
	$\sigma^0_{Ri}/R_{i,0}$ (%)	$\Delta\sigma^0_{Ri}/R_{i,0}$ (%)	$\sigma^0_{Ri}/R_{i,0}$ (%)	$\Delta\sigma^0_{Ri}/R_{i,0}$ (%)
k_∞	4.571E-01	8.966E-03	4.660E-01	9.126E-03
$\Sigma_{t,1}$	9.043E-01	2.683E-02	9.119E-01	2.714E-02
$\Sigma_{t,2}$	2.901E-01	6.408E-03	2.900E-01	6.405E-03
$\Sigma_{a,1}$	8.209E-01	2.152E-02	8.333E-01	2.201E-02
$\Sigma_{a,2}$	2.780E-01	6.439E-03	2.798E-01	6.483E-03
$\nu\Sigma_{f,1}$	5.396E-01	1.202E-02	5.412E-01	1.202E-02
$\nu\Sigma_{f,2}$	3.692E-01	9.172E-03	3.699E-01	9.209E-03
$\Sigma_{s,1,1}$	9.023E-01	2.672E-02	9.101E-01	2.702E-02
$\Sigma_{s,1,2}$	1.180E+00	3.445E-02	1.193E+00	3.488E-02
$\Sigma_{s,2,1}$	4.812E-01	1.078E-02	5.706E-01	1.376E-02
$\Sigma_{s,2,2}$	3.181E-01	7.042E-03	3.180E-01	6.998E-03

TABLE IV

Uncertainties for TMI-1 Assembly Applying ν_t Covariance Matrix of ^{235}U-ν

Response	HZP Conditions		HFP Conditions	
	$\sigma^0_{Ri}/R_{i,0}$ (%)	$\Delta\sigma^0_{Ri}/R_{i,0}$ (%)	$\sigma^0_{Ri}/R_{i,0}$ (%)	$\Delta\sigma^0_{Ri}/R_{i,0}$ (%)
k_∞	7.085E-01	1.981E-02	7.122E-01	1.974E-02
$\Sigma_{t,1}$	9.043E-01	2.683E-02	9.119E-01	2.714E-02
$\Sigma_{t,2}$	2.901E-01	6.408E-03	2.900E-01	6.405E-03
$\Sigma_{a,1}$	8.209E-01	2.152E-02	8.333E-01	2.201E-02
$\Sigma_{a,2}$	2.780E-01	6.439E-03	2.798E-01	6.483E-03
$\nu\Sigma_{f,1}$	6.499E-01	1.396E-02	6.511E-01	1.396E-02
$\nu\Sigma_{f,2}$	7.499E-01	2.323E-02	7.503E-01	2.323E-02
$\Sigma_{s,1,1}$	9.023E-01	2.672E-02	9.101E-01	2.702E-02
$\Sigma_{s,1,2}$	1.180E+00	3.445E-02	1.193E+00	3.488E-02
$\Sigma_{s,2,1}$	4.812E-01	1.078E-02	5.706E-01	1.376E-02
$\Sigma_{s,2,2}$	3.181E-01	7.042E-03	3.180E-01	6.998E-03

responses, including k_∞, $\nu\Sigma_{f,1}$, and $\nu\Sigma_{f,2}$. Third, the relative uncertainties of the TMI-1 assembly at both HZP and HFP conditions, introduced by the uncertainties of all analyzed nuclides and cross sections as shown in Table II, could be up to about (4.7 ± 0.09)‰ (with application of the ν_p covariance matrix for ^{235}U-ν) or (7.1 ± 0.20)‰ (with application of the ν_t covariance matrix for ^{235}U-ν) for k_∞. For the two-group macroscopic cross sections, the smallest relative uncertainty is about (2.9 ± 0.06)‰ (for the total cross section of thermal group $\Sigma_{t,2}$), while the largest one could be up to about (11.9 ± 0.34)‰ (for the scattering cross section from the fast group to the thermal group $\Sigma_{s,1,2}$). These uncertainties are large and significant for neutronics calculations and cannot be ignored.

To find the most significant uncertainty contribution nuclides for the response uncertainties of the TMI-1 assembly at both HZP and HFP conditions, detailed comparisons of uncertainties introduced by every single nuclide are shown in Fig. 3.

From the uncertainty contribution comparisons shown in Fig. 3, it can be observed that the uncertainty contributions of each single nuclide for the TMI-1 assembly at both HZP and HFP conditions are consistent, which means that the same nuclide would introduce almost the same contributions to the response uncertainties for both HZP and HFP conditions. In addition, ^{235}U, ^{238}U, ^{16}O, and ^{1}H are the four most significant nuclides, or contributors, to the uncertainties of k_∞ and the two-group macroscopic cross sections.

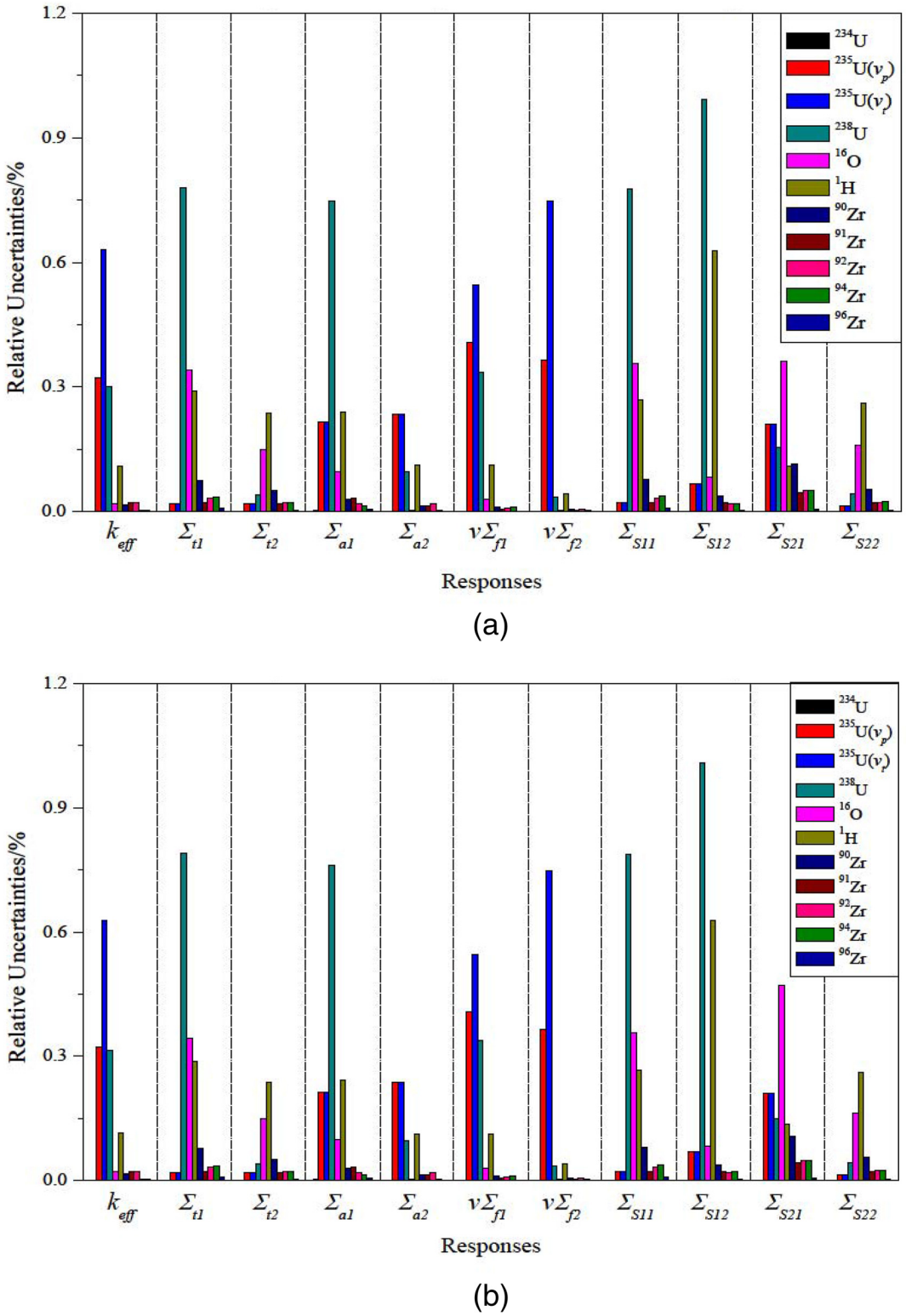

Fig. 3. Uncertainty contributions by nuclides for the TMI-1 assembly. (a) HZP conditions. (b) HFP conditions.

For a more detailed and deeper analysis, to determine the uncertainty contributions of each type of cross section for the four most significant nuclides analyzed, the response uncertainties introduced by every type of cross section analyzed for the four most significant nuclides are compared and shown in Figs. 4 through 7.

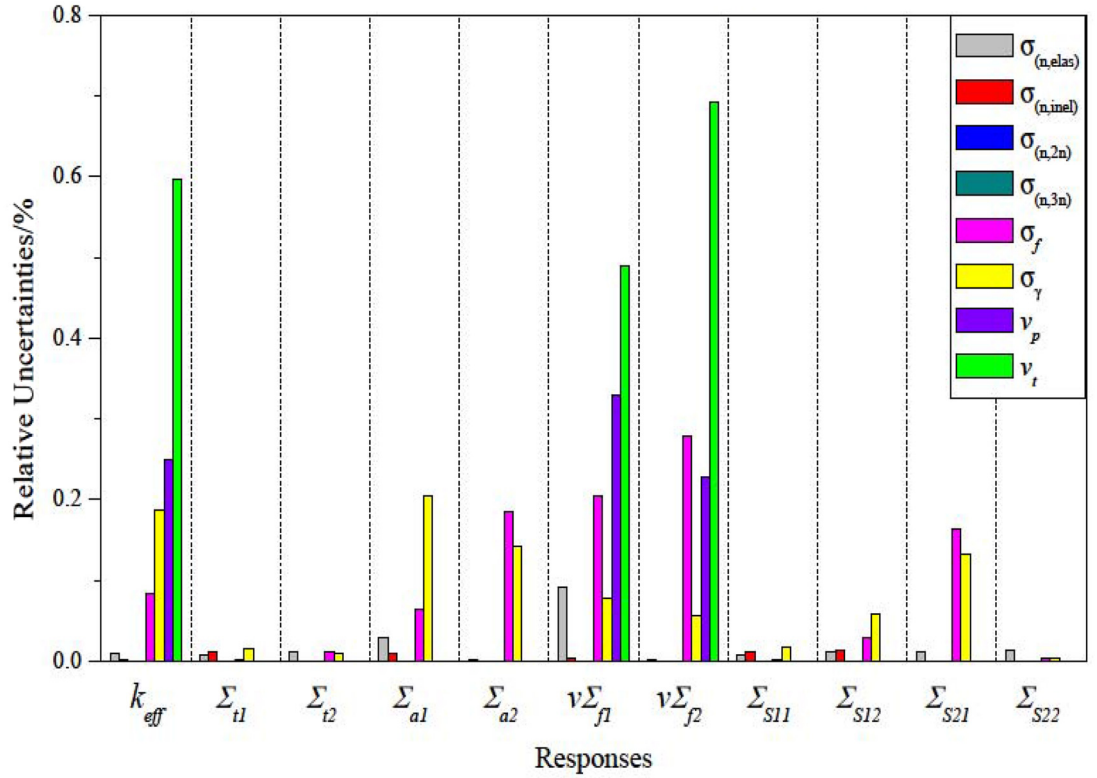

(a)

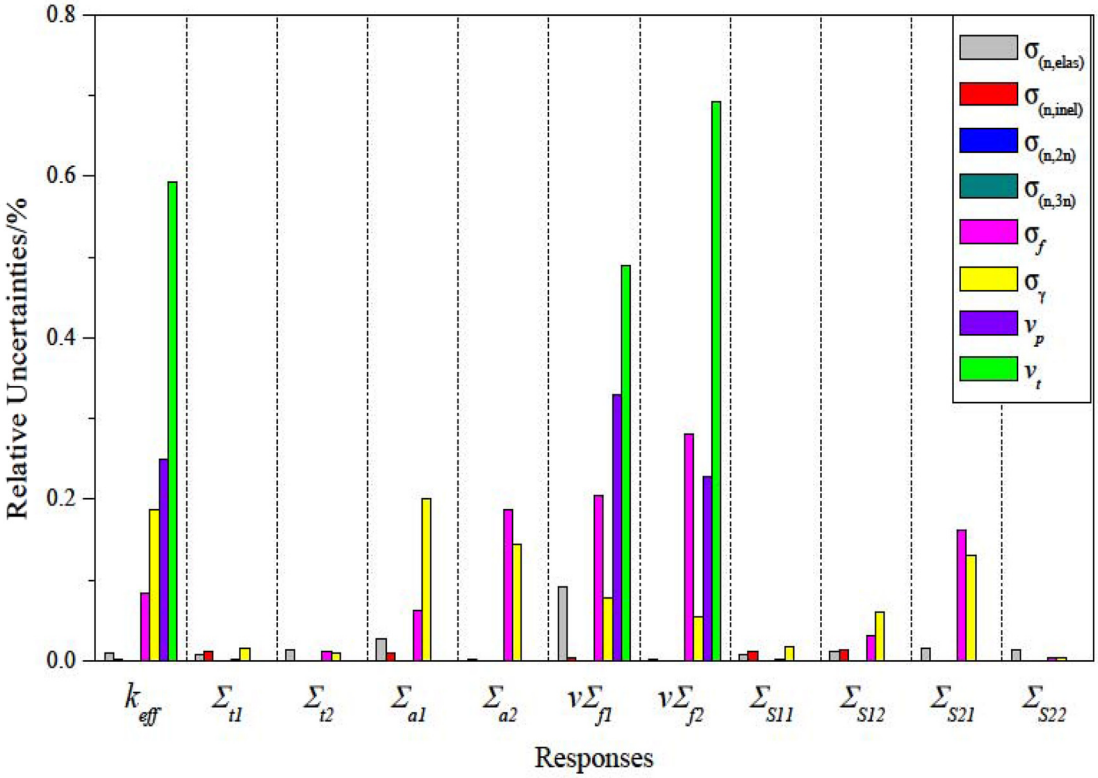

(b)

Fig. 4. Cross-section contribution comparisons of ^{235}U. (a) HZP conditions. (b) HFP conditions.

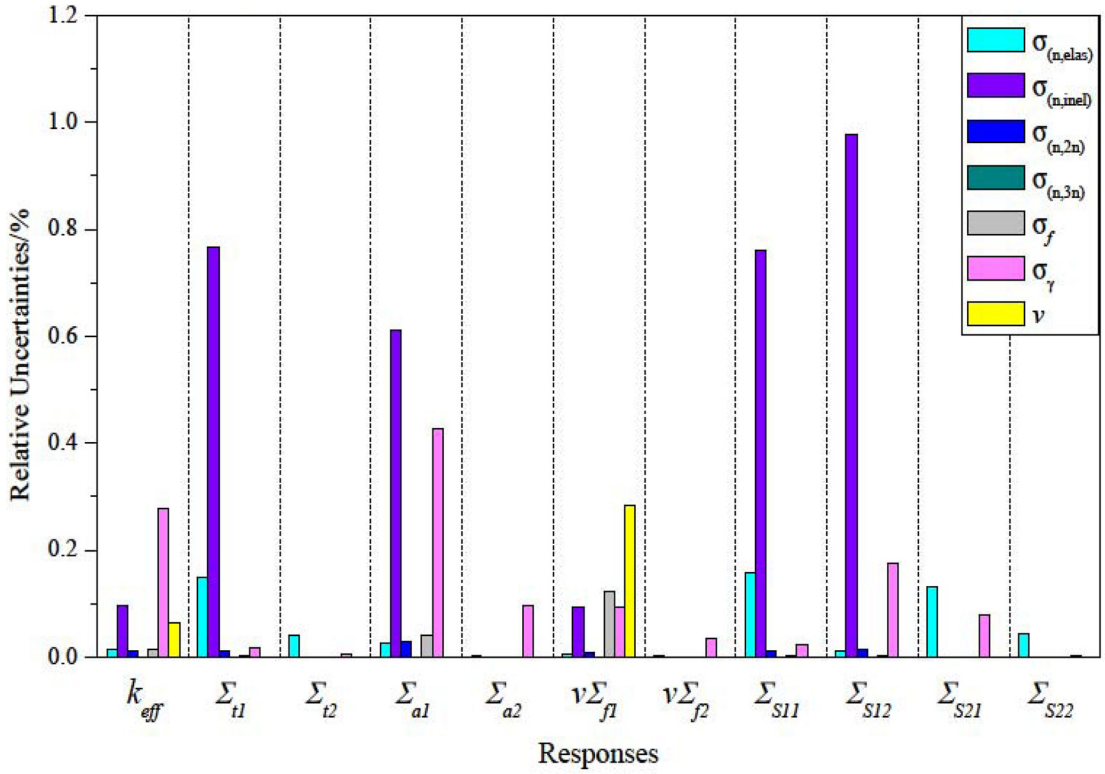

(a)

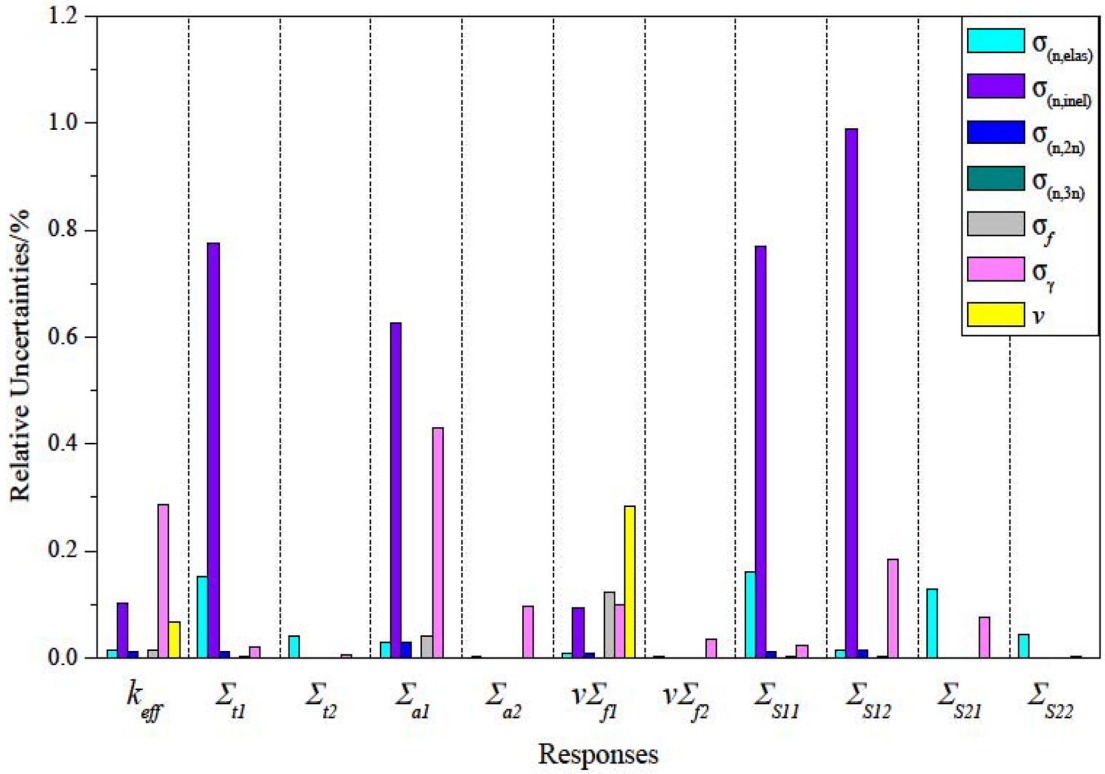

(b)

Fig. 5. Cross-section contribution comparisons of ^{238}U. (a) HZP conditions. (b) HFP conditions.

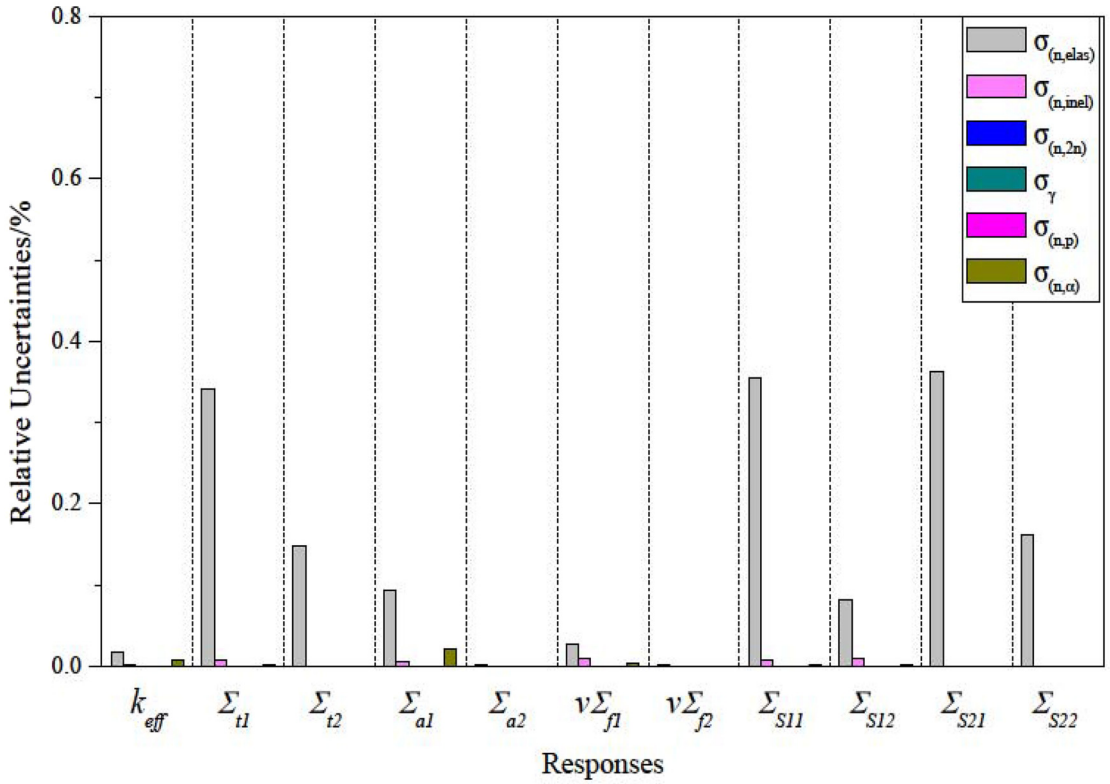

(a)

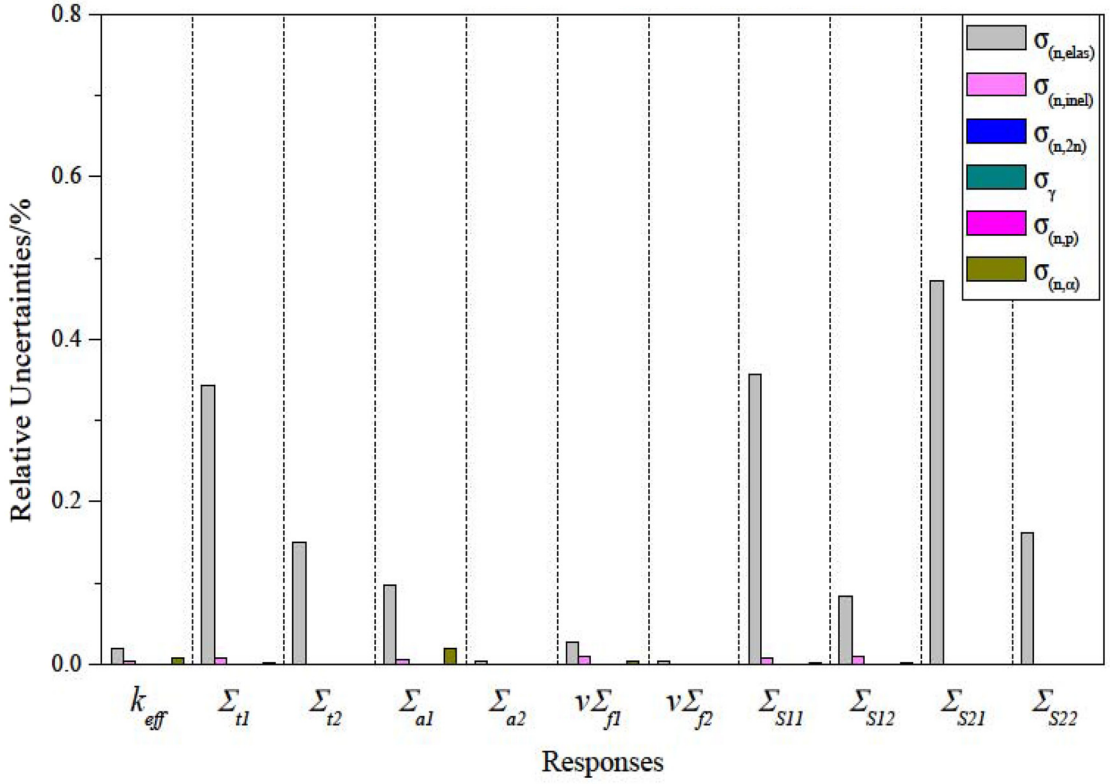

(b)

Fig. 6. Cross-section contribution comparisons of ^{16}O. (a) HZP conditions. (b) HFP conditions.

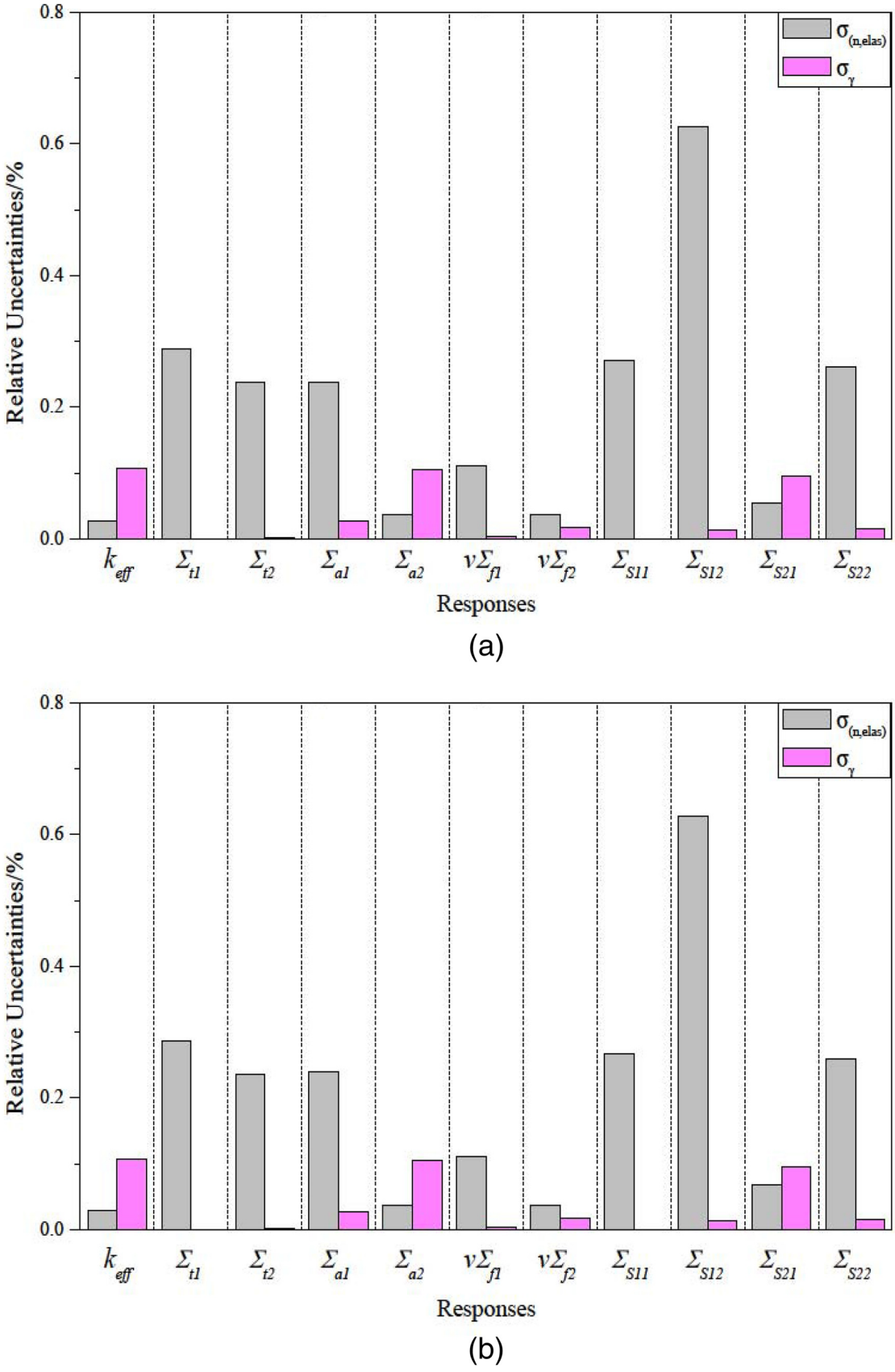

Fig. 7. Cross-section contribution comparisons of ^{1}H. (a) HZP conditions. (b) HFP conditions.

According to the comparisons for the uncertainty contribution of cross sections shown in Figs. 4 through 7, it can be observed that for ^{235}U, the three most significant cross-section contributors are ν (both ν_p and ν_t), σ_f, and σ_γ. For ^{238}U, the four most significant cross-section contributors are σ_γ, $\sigma_{(n,inel)}$, $\sigma_{(n,elas)}$, and ν. For ^{16}O, the most significant cross section is $\sigma_{(n,elas)}$. For ^{1}H, $\sigma_{(n,elas)}$ and σ_γ are the two most significant cross-section contributors. Moreover, through the detailed contribution analysis for all types of cross sections of all the analyzed nuclides, the five most significant cross-section contributors for each response uncertainty of the TMI-1 assembly at both HZP and HFP conditions are determined, as shown in Tables V and VI, respectively.

It can be observed from the uncertainty results shown in Tables V and VI that the five most significant cross-section contributors for the response uncertainties of the TMI-1 assembly almost consist of the most significant cross sections of the four most significant nuclides analyzed above. For the other nuclides analyzed in this paper, $\sigma_{(n,elas)}$ of ^{90}Zr and ^{94}Zr has some notable contributions to the uncertainties of some responses, including $\Sigma_{t,1}$, $\Sigma_{t,2}$, $\Sigma_{s,1,1}$, $\Sigma_{s,2,1}$, and $\Sigma_{s,2,2}$.

In conclusion for this section, total uncertainty analyses have been performed for the TMI-1 assembly, at both HZP and HFP conditions, and detailed analyses of the uncertainty sources of nuclides and cross sections have been performed. The most significant nuclides and cross-section types have been determined in this paper, which

TABLE V

The Five Most Significant Cross-Section Contributors of Responses at HZP

Response	Nuclide	Cross Section	$\sigma^0_{Ri}/R_{i,0}$ (%)	$\Delta\sigma^0_{Ri}/R_{i,0}$ (%)	Response	Nuclide	Cross Section	$\sigma^0_{Ri}/R_{i,0}$ (%)	$\Delta\sigma^0_{Ri}/R_{i,0}$ (%)
k_∞	^{235}U	ν_t	5.958E-01	1.966E-02	$\nu\Sigma_{f,2}$	^{235}U	ν_t	6.917E-01	2.312E-02
	^{238}U	σ_γ	2.781E-01	7.506E-03		^{235}U	σ_f	2.789E-01	8.550E-03
	^{235}U	ν_p	2.489E-01	6.506E-03		^{235}U	ν_p	2.286E-01	6.439E-03
	^{235}U	σ_γ	1.866E-01	5.841E-03		^{235}U	σ_γ	5.628E-02	1.856E-03
	^{1}H	σ_γ	1.073E-01	2.733E-03		^{1}H	$\sigma_{(n,elas)}$	3.799E-02	9.249E-04
$\Sigma_{t,1}$	^{238}U	$\sigma_{(n,inel)}$	7.660E-01	2.665E-02	$\Sigma_{s,1,1}$	^{238}U	$\sigma_{(n,inel)}$	7.614E-01	2.651E-02
	^{16}O	$\sigma_{(n,elas)}$	3.420E-01	1.000E-02		^{16}O	$\sigma_{(n,elas)}$	3.557E-01	1.041E-02
	^{1}H	$\sigma_{(n,elas)}$	2.890E-01	7.641E-03		^{1}H	$\sigma_{(n,elas)}$	2.702E-01	7.143E-03
	^{238}U	$\sigma_{(n,elas)}$	1.490E-01	5.649E-03		^{238}U	$\sigma_{(n,elas)}$	1.568E-01	5.952E-03
	^{90}Zr	$\sigma_{(n,elas)}$	6.950E-02	1.847E-03		^{90}Zr	$\sigma_{(n,elas)}$	7.311E-02	1.943E-03
$\Sigma_{t,2}$	^{1}H	$\sigma_{(n,elas)}$	2.374E-01	6.048E-03	$\Sigma_{s,1,2}$	^{238}U	$\sigma_{(n,inel)}$	9.774E-01	3.399E-02
	^{16}O	$\sigma_{(n,elas)}$	1.486E-01	4.288E-03		^{1}H	$\sigma_{(n,elas)}$	6.269E-01	1.645E-02
	^{90}Zr	$\sigma_{(n,elas)}$	4.979E-02	1.716E-03		^{238}U	σ_γ	1.748E-01	5.152E-03
	^{238}U	$\sigma_{(n,elas)}$	3.915E-02	1.007E-03		^{16}O	$\sigma_{(n,elas)}$	8.098E-02	2.407E-03
	^{94}Zr	$\sigma_{(n,elas)}$	2.236E-02	5.659E-04		^{235}U	σ_γ	5.857E-02	1.796E-03
$\Sigma_{a,1}$	^{238}U	$\sigma_{(n,inel)}$	6.101E-01	2.084E-02	$\Sigma_{s,2,1}$	^{16}O	$\sigma_{(n,elas)}$	3.623E-01	1.045E-02
	^{238}U	σ_γ	4.264E-01	1.226E-02		^{235}U	σ_f	1.636E-01	4.940E-03
	^{1}H	$\sigma_{(n,elas)}$	2.383E-01	6.393E-03		^{238}U	$\sigma_{(n,elas)}$	1.326E-01	3.599E-03
	^{235}U	σ_γ	2.051E-01	6.115E-03		^{235}U	σ_γ	1.321E-01	4.617E-03
	^{16}O	$\sigma_{(n,elas)}$	9.368E-02	2.756E-03		^{90}Zr	$\sigma_{(n,elas)}$	1.135E-01	3.911E-03
$\Sigma_{a,2}$	^{235}U	σ_f	1.853E-01	5.693E-03	$\Sigma_{s,2,2}$	^{1}H	$\sigma_{(n,elas)}$	2.617E-01	6.669E-03
	^{235}U	σ_γ	1.431E-01	4.862E-03		^{16}O	$\sigma_{(n,elas)}$	1.610E-01	4.646E-03
	^{1}H	σ_γ	1.058E-01	2.710E-03		^{90}Zr	$\sigma_{(n,elas)}$	5.442E-02	1.876E-03
	^{238}U	σ_γ	9.538E-02	2.722E-03		^{238}U	$\sigma_{(n,elas)}$	4.260E-02	1.095E-03
	^{1}H	$\sigma_{(n,elas)}$	3.746E-02	9.502E-04		^{94}Zr	$\sigma_{(n,elas)}$	2.444E-02	6.183E-04
$\nu\Sigma_{f,1}$	^{235}U	ν_t	4.896E-01	1.184E-02					
	^{235}U	ν_p	3.295E-01	7.137E-03					
	^{238}U	ν	2.822E-01	1.142E-02					
	^{235}U	σ_f	2.055E-01	4.825E-03					
	^{238}U	σ_f	1.230E-01	4.380E-03					

TABLE VI

The Five Most Significant Cross-Section Contributors of Responses at HFP

Response	Nuclide	Cross Section	$\sigma^0_{Ri}/R_{i,0}$ (%)	$\Delta\sigma^0_{Ri}/R_{i,0}$ (%)	Response	Nuclide	Cross Section	$\sigma^0_{Ri}/R_{i,0}$ (%)	$\Delta\sigma^0_{Ri}/R_{i,0}$ (%)
k_∞	^{235}U	ν_t	5.936E-01	1.957E-02	$\nu\Sigma_{f,2}$	^{235}U	ν_t	6.916E-01	2.312E-02
	^{238}U	σ_γ	2.878E-01	7.725E-03		^{235}U	σ_f	2.802E-01	8.596E-03
	^{235}U	ν_p	2.495E-01	6.510E-03		^{235}U	ν_p	2.286E-01	6.439E-03
	^{235}U	σ_γ	1.869E-01	5.866E-03		^{235}U	σ_γ	5.540E-02	1.831E-03
	^{1}H	σ_γ	1.073E-01	2.733E-03		^{1}H	$\sigma_{(n,elas)}$	3.770E-02	9.519E-04
$\Sigma_{t,1}$	^{238}U	$\sigma_{(n,inel)}$	7.740E-01	2.695E-02	$\Sigma_{s,1,1}$	^{238}U	$\sigma_{(n,inel)}$	7.699E-01	2.682E-02
	^{16}O	$\sigma_{(n,elas)}$	3.434E-01	1.005E-02		^{16}O	$\sigma_{(n,elas)}$	3.575E-01	1.047E-02
	^{1}H	$\sigma_{(n,elas)}$	2.863E-01	7.566E-03		^{1}H	$\sigma_{(n,elas)}$	2.674E-01	7.069E-03
	^{238}U	$\sigma_{(n,elas)}$	1.512E-01	5.742E-03		^{238}U	$\sigma_{(n,elas)}$	1.594E-01	6.051E-03
	^{90}Zr	$\sigma_{(n,elas)}$	7.081E-02	1.884E-03		^{90}Zr	$\sigma_{(n,elas)}$	7.446E-02	1.982E-03
$\Sigma_{t,2}$	^{1}H	$\sigma_{(n,elas)}$	2.356E-01	5.979E-03	$\Sigma_{s,1,2}$	^{238}U	$\sigma_{(n,inel)}$	9.899E-01	3.443E-02
	^{16}O	$\sigma_{(n,elas)}$	1.493E-01	4.309E-03		^{1}H	$\sigma_{(n,elas)}$	6.281E-01	1.646E-02
	^{90}Zr	$\sigma_{(n,elas)}$	5.090E-02	1.755E-03		^{238}U	σ_γ	1.844E-01	5.436E-03
	^{238}U	$\sigma_{(n,elas)}$	4.009E-02	1.032E-03		^{16}O	$\sigma_{(n,elas)}$	8.283E-02	2.461E-03
	^{94}Zr	$\sigma_{(n,elas)}$	2.286E-02	5.788E-04		^{235}U	σ_γ	6.018E-02	1.850E-03
$\Sigma_{a,1}$	^{238}U	$\sigma_{(n,elas)}$	6.252E-01	2.137E-02	$\Sigma_{s,2,1}$	^{16}O	$\sigma_{(n,elas)}$	4.717E-01	1.362E-02
	^{238}U	σ_γ	4.291E-01	1.233E-02		^{235}U	σ_f	1.624E-01	4.892E-03
	^{1}H	$\sigma_{(n,elas)}$	2.407E-01	6.473E-03		^{235}U	σ_γ	1.317E-01	4.610E-03
	^{235}U	σ_γ	2.009E-01	6.007E-03		^{238}U	$\sigma_{(n,elas)}$	1.289E-01	3.495E-03
	^{16}O	$\sigma_{(n,elas)}$	9.675E-02	2.844E-03		^{90}Zr	$\sigma_{(n,elas)}$	1.066E-01	3.665E-03
$\Sigma_{a,2}$	^{235}U	σ_f	1.865E-01	5.735E-03	$\Sigma_{s,2,2}$	^{1}H	$\sigma_{(n,elas)}$	2.602E-01	6.604E-03
	^{235}U	σ_γ	1.442E-01	4.894E-03		^{16}O	$\sigma_{(n,elas)}$	1.622E-01	4.680E-03
	^{1}H	σ_γ	1.058E-01	2.710E-03		^{90}Zr	$\sigma_{(n,elas)}$	5.569E-02	1.920E-03
	^{238}U	σ_γ	9.616E-02	2.741E-03		^{238}U	$\sigma_{(n,elas)}$	4.367E-02	1.123E-03
	^{1}H	$\sigma_{(n,elas)}$	3.755E-02	9.484E-04		^{94}Zr	$\sigma_{(n,elas)}$	2.501E-02	6.333E-04
$\nu\Sigma_{f,1}$	^{235}U	ν_t	4.896E-01	1.184E-02					
	^{235}U	ν_p	3.296E-01	7.139E-03					
	^{238}U	ν	2.821E-01	1.141E-02					
	^{235}U	σ_f	2.055E-01	4.823E-03					
	^{238}U	σ_f	1.229E-01	4.377E-03					

indicates the most significant nuclides and cross sections for the accuracy of neutronics calculations.

IV. CONCLUSIONS

In this paper, total uncertainty analyses have been performed for the TMI-1 assembly, at both HZP and HFP conditions, using the home-developed code UNICORN based on a statistical sampling method. In the total uncertainty analyses, a 172-group cross-section covariance library based on ENDF/B-VII.1 is produced and applied to generate the multigroup microscopic cross-section samples with the improved multigroup cross-section perturbation model. The uncertainties of k_∞ and two-group macroscopic cross sections have been calculated, and detailed analyses of the contributions of ten main nuclides contained in the composition materials and the corresponding 48 cross sections have been carried out. From the uncertainty results of the TMI-1 assembly at both HZP and HFP conditions, some conclusions can be obtained.

First, the total relative uncertainty for k_∞ could be up to about (4.7 ± 0.09)‰ (with application of the ν_p covariance matrix for ^{235}U-ν) or (7.1 ± 0.20)‰ (with application of the ν_t covariance matrix for ^{235}U-ν). The smallest relative uncertainty of the two-group macroscopic cross sections is about (2.9 ± 0.06)‰ (for $\Sigma_{t,2}$), while the largest can be up to about (11.9 ± 0.34)‰ (for $\Sigma_{s,1,2}$). Moreover, the uncertainties for the responses of the TMI-1 assembly at HFP conditions are slightly larger than those at the HZP conditions.

Second, the response uncertainties introduced by ^{235}U ν could be notably different by applying the covariance matrix of ν_p and ν_t. The covariance matrix of ^{235}U ν_t would introduce larger uncertainties to the responses than those for ν_p, especially for the responses k_∞, $\nu\Sigma_{f,1}$, and $\nu\Sigma_{f,2}$. This should be noted when performing an uncertainty analysis for ν of ^{235}U.

Third, ^{235}U, ^{238}U, ^{16}O, and ^{1}H are the four most significant nuclide uncertainty sources for the TMI-1 assembly at both HZP and HFP conditions. In detail, it has been observed that for ^{235}U, the most significant cross-section uncertainty sources are ν, σ_f, and σ_γ. For ^{238}U, they are σ_γ, $\sigma_{(n,inel)}$, $\sigma_{(n,elas)}$, and ν. For ^{16}O, it is $\sigma_{(n,elas)}$. For ^{1}H, they are $\sigma_{(n,elas)}$ and σ_γ. For the other nuclides analyzed in this paper, $\sigma_{(n,elas)}$ of ^{90}Zr and ^{94}Zr has some notable contributions to the uncertainties of some responses, including $\Sigma_{t,1}$, $\Sigma_{t,2}$, $\Sigma_{s,1,1}$, $\Sigma_{s,2,1}$, and $\Sigma_{s,2,2}$.

In this context, the response uncertainties of the TMI-1 assembly at both HZP and HFP conditions, introduced by the main nuclides and types of cross sections of the composition materials, are significant and nonnegligible for neutronics calculations.

Acknowledgments

This work is supported by the National Natural Science Foundation of China (grant 11522544).

References

1. K. IVANOV et al., "Benchmarks for Uncertainty Analysis in Modeling (UAM) for the Design, Operation and Safety Analysis of LWRs," NEA/NSC/DOC(2013)7, Organisation for Economic Cooperation and Development/Nuclear Energy Agency (2013).
2. M. PUSA, "Incorporating Sensitivity and Uncertainty Analysis to a Lattice Physics Code with Application to CASMO-4," *Ann. Nucl. Energy*, **40**, 153 (2012); http://dx.doi.org/10.1016/j.anucene.2011.10.013.
3. B. T. REARDEN, L. M. PETRIE, and M. A. JESSEE, "SAMS: Sensitivity Analysis Module for SCALE," ORNL/TM-2005/39, Version 6, Vol. II, Sec. F22, Oak Ridge National Laboratory (2009).
4. M. R. BALL, D. R. NOVOG, and J. C. LUXAT, "Analysis of Implicit and Explicit Lattice Sensitivity Using DRAGON," *Nucl. Eng. Des.*, **265**, 1 (2013); http://dx.doi.org/10.1016/j.nucengdes.2013.07.011.
5. B. FOAD and T. TAKEDA, "Sensitivity and Uncertainty Analysis for UO_2 and MOX Fueled PWR Cells," *Ann. Nucl. Energy*, **75**, 595 (2015); http://dx.doi.org/10.1016/j.anucene.2014.08.068.
6. M. DION and G. MARLEAU, "Resonance Self-Shielding Effects on Eigenvalue Sensitivity," *Proc. M&C 2013*, Sun Valley, Idaho, May 5–9, 2013.
7. K. KINOSHITA, A. YAMAMOTO, and T. ENDO, "Uncertainty Quantification of BWR Core Characteristics Using Latin Hypercube Sampling Method," *Proc. PHYSOR 2014*, Kyoto, Japan, September 28–October 3, 2014.
8. J. C. HELTON et al., "Survey of Sampling-Based Methods for Uncertainty and Sensitivity Analysis," *Reliab. Eng. Syst. Saf.*, **91**, 1175 (2006); http://dx.doi.org/10.1016/j.ress.2005.11.017.
9. M. WILLIAMS et al., "Development of a Statistical Sampling Method for Uncertainty Analysis with SCALE," *Proc. PHYSOR 2012*, Knoxville, Tennessee, April 15–20, 2012.
10. T. TAKEDA, K. ASANO, and T. KITADA, "Sensitivity Analysis Based on Transport Theory," *J. Nucl. Sci. Technol.*, **43**, *7*, 743 (2006); http://dx.doi.org/10.1080/18811248.2006.9711156.
11. G. E. B. ARCHER, A. SALTELLI, and I. M. SOBOL, "Sensitivity Measures, Anova-Like Techniques and the Use of Bootstrap," *J. Stat. Comput. Simul.*, **58**, 99 (1997); http://dx.doi.org/10.1080/00949659708811825.
12. G. MARLEAU, A. HÉBERT, and R. ROY, "A User Guide for DRAGON Version 5," IGE-335, Institut de genie nucléaire (2013).
13. F. LESZCZYNSKI, D. L. ALDAMA, and A. TRKOV, "WIMSD-4 Library Update: Final Report of a Coordinated Research Project," STI/PUB/1246, International Atomic Energy Agency (2007).
14. C. WAN et al., "Code Development for Eigenvalue Total Sensitivity Analysis and Total Uncertainty Analysis," *Ann. Nucl. Energy*, **85**, 788 (2015); http://dx.doi.org/10.1016/j.anucene.2015.06.036.
15. R. E. MacFARLANE et al., "The NJOY Nuclear Data Processing System Version 2012," LA-UR-12-27079, Los Alamos National Security (2012).
16. A. H. SOLÍS, C. DEMAZIÈRE, and C. EKBERG, "Uncertainty and Sensitivity Analyses Applied to the DRAGONv4.05 Code Lattice Calculations and Based on JENDL-4 Data," *Ann. Nucl. Energy*, **57**, 230 (2013); http://dx.doi.org/10.1016/j.anucene.2013.01.061.
17. J. C. HELTON and F. J. DAVIS, "Latin Hypercube Sampling and the Propagation of Uncertainty in Analysis of Complex System," SAND2001-0417, Sandia National Laboratories (2002).
18. S. S. WILKS, "Determination of Sample Size for Setting Tolerance Limits," *Ann. Math. Stat.*, **12**, 91 (1941); http://dx.doi.org/10.1214/aoms/1177731788.